



# Metakaolin-based geopolymers for stone conservation: preliminary results on alkaline activation

Sophie van Roosmale<sup>1,2</sup>, Tim De Kock<sup>1</sup>, and Johan Blom<sup>2</sup>

<sup>1</sup>Antwerp Cultural Heritage Sciences (ARCHES), Faculty of Design Sciences,  
University of Antwerp, Blindestraat 9, 2000 Antwerp, Belgium

<sup>2</sup>Energy and Materials in Infrastructure and Buildings (EMIB), Faculty of Applied Engineering,  
Antwerp, Groenenborgerlaan 171, 2020 Antwerp, Belgium

**Correspondence:** Sophie van Roosmale (sophie.vanroosmale@uantwerpen.be)

Received: 15 July 2022 – Revised: 13 October 2022 – Accepted: 10 January 2023 – Published: 27 January 2023

**Abstract.** Geopolymers are inorganic and versatile alternative binder. They exist in a wide range, varying from a material which behaves like mortars to a material with properties like ceramics. This makes them a potentially innovative alternative to repair mortars. In this research the activation of metakaolin-based geopolymers is explored in the context of stone conservation. A set of reactivity tests are performed to evaluate activators and compatibility with a lime-based binder. The physico-chemical properties of the binder are investigated, in combination with low proportions of standardized aggregates of marl powder, limestone powder and quartz sand. The most promising mixtures absorb water relatively slowly due to the relative small pore sizes. The samples have a high open porosity and therefore a lower density when compared to results found in literature from geopolymers with aggregate, but the results are comparable to geopolymers without aggregates. The compressive strength is comparable to currently used repair mortars. This study shows that metakaolin with lime-based binders could be investigated in the future as alternative binder in stone repair mortars.

## 1 Introduction

Stone is a traditional material used in monuments worldwide. Although stone is associated with longevity, it is not an inert material. It undergoes surface processes leading to degradation (functional and aesthetical). Current methods in conservation include the reconstruction of missing parts with repair mortars (Isebaert et al., 2014, 2019). However, repair mortars

not always show good technical and aesthetical compatibility with the stone substrate (Isebaert et al., 2014). A recent study of commercial repair mortars evidenced distinct chemical and mechanical properties for each mortar in comparison to different substrates (Lubelli et al., 2019).

In this research, the use of geopolymers as alternative binder for repair mortars is investigated. Geopolymers can be tailor-made and have several (environmental) advantages compared to Portland cement (Pereira et al., 2018). They are considered as a subset of alkali-activated materials (AAM), manufactured by a chemical process like cements but have more similarities with ceramic materials, including the form of the crystalline structure (Provis et al., 2018). Geopolymers are inorganic, stable in different pH levels, obtainable from accessible raw materials and easily processable (Cong et al., 2021; Pouhet, 2015). There are different types of geopolymers, each with their specific properties that can be modified by aggregates (Cong et al., 2021). Here, the focus is on metakaolin-based geopolymers. Metakaolin is the dehydroxylated product of calcined kaolin clay, calcinated at low temperatures (500 to 800 °C). It reacts with alkaline activators in the presence of moisture to a geopolymer (Pouhet, 2015; Van Deventer et al., 2009; Alventosa et al., 2021; Siddique et al., 2009).

Initial studies have looked into the possible application of metakaolin geopolymers in heritage conservation (Pagnotta et al., 2020; Geraldès et al., 2016; Ricciotti et al., 2017). Clausi et al. (2016a, b) investigated the use of metakaolin-based geopolymers in the restoration of ornamental stones and the effect of sandstone, dolomite and limestone as aggregates with Na<sub>2</sub>O : SiO<sub>2</sub> in water (14.37 wt % : 29.54 wt %, 2016a, b).

H<sub>2</sub>O 56.09 wt %) as an activator. Through SEM-EDS and FESEM-EDAX analysis they proved a reaction has occurred to a very low extent between the calcium from the stones and the geopolymer. The concentration of calcium was too low to form calcium silicate hydrate (CSH) gels, but the adhesion was improved (Granizo et al., 2002). Alonso et al. (2001) have investigated the effect of Ca(OH)<sub>2</sub> aggregate on a metakaolin-based geopolymer with NaOH as an activator. They have found that CSH gel is formed, but only when the activator has a lower alkalinity. Allali et al. (2016) further explained how Ca(OH)<sub>2</sub> reacts with the metakaolin and Na<sub>2</sub>O : SiO<sub>2</sub> in water (14.37 wt % : 29.54 wt %, H<sub>2</sub>O 56.09 wt %) as activator through IR spectra. All calcium is used in Si-O-Ca compounds and no carbonates are formed.

Furthermore, metakaolin has been used as a pozzolan for lime based restoration mortars, because it can improve mechanical behaviour and durability (Dimou et al., 2022). Liu et al. (2020) showed with XRD both a pozzolanic and a carbonation reaction happen in a lime mortar sample with metakaolin, resulting in increased compressive strength and porosity.

In order to explore the effect of Ca(OH)<sub>2</sub> as an activator for a metakaolin-based geopolymer, experiments have been performed with different ratios of Ca(OH)<sub>2</sub>, as limewater and as a slurry. The setting will be compared to low molarities of typical activators like NaOH and KOH. Although the literature states that high molarity of activators is required (Van Deventer et al., 2009; Alonso et al., 2001; Pacheco-Tornal et al., 2015), the decision was made to use low concentrations, because of safety considerations for the users (Siddique et al., 2009). Even more important, a higher concentration of alkalis leads to a higher risk of efflorescence (Longhi et al., 2020). Following this first test phase, the effect of the addition of standardised aggregates on the geopolymer with a combination of limewater and slurry has been investigated.

## 2 Materials and methods

### 2.1 Materials used in the design phase of the samples

The samples were designed using metakaolin (MK) Agrical® M1000 (Imerys, Clérac, France) with a 95 % purity and specific surface area of 20 m<sup>2</sup> g<sup>-1</sup> as source of aluminosilicate. Three alkaline activators, NaOH pellets from VWR (98 % purity dissolved in water), KOH from Merck (85 % purity dissolved in water) and Ca(OH)<sub>2</sub> from Sigma-Aldrich (95 % purity as limewater/slurry), were used in different concentrations. The Heidolph RZR 2102 overhead blade mixer with a TR 21 Radial-Flow Impeller (50 mm) stirring tool is used to mix the different samples at two different speeds: 250 rpm for 1 min and 350 rpm for 2 min with an accuracy of ± 5 rpm, to ensure homogeneity. The mixtures were then poured into cylindric moulds (height 50 mm, diameter of 35 mm) and sealed to cure at room temperature. Af-

ter approximately 48 h the samples were removed from their mould. The first part of this research, focusses on the reactivity of the samples (Table 1). The next part focusses on the effect of aggregates on the reactivity and on the mechanical properties (Table 2).

Sample “30Ca4” is selected (from batch 1) to which the different aggregates are being added. The aggregates are quartz sand (M34), limestone powder (Ankerfill 125) and marl powder (Inducal 105) from Sibelco (Belgium). First, all the dry components are being mixed by hand for 1 min and then the Ca(OH)<sub>2</sub> is added as the activator. The samples are mixed and poured in the same way as the first batch. After approximately 48 h the samples were removed from their mould.

### 2.2 Reactivity tests

Three tests were performed to examine the reactivity. First, the degree of setting of the samples was evaluated by looking for visual changes in the shape of the samples as soon as they were removed from the mould. In the second test, the samples were partially immersed in demineralized water for 4 h at room temperature and with atmospheric pressure to see if there was a binding effect. Samples that showed enough binding were scanned with a Confocal Laser Scanning Microscope (CLSM, Keyence) and with a Scanning Electron Microscope (SEM, COXEM EM-30plus) instrument with a voltage of 15–25 kV, to evaluate homogeneity and to look for defects in the structure like non-reacted and loose powder or layering.

### 2.3 Physico-mechanical properties

The open porosity was determined by the Archimedes principle (EN 1936:2006, 2007) on samples with a diameter < 1 cm. Pore size distribution was measured through mercury intrusion porosimetry (Autopore IV 9500 V1.09), with a maximum head pressure of 4.4500 psia. The contact angle and surface tension used for calculations were 130° and 485 dynes cm<sup>-1</sup>.

Capillary water absorption was quantified according to EN 1925:1999 (1999) using cylindrical samples with nominal height and diameter of 40.0 and 32.0 mm. The dry samples were partially immersed in 3.0 mm of water in a sealed container to prevent water evaporation. Subsequently, the samples are fully immersed in water and weighed after another 48 h to calculate the atmospheric saturation. The bulk density was calculated by dimensional measurement and the weight of the samples. The uniaxial compressive strength and strain was measured after 40 d of curing with a Uniframe 50 KN device with a test speed of 50 N s<sup>-1</sup>, following the EN 1015-11 (1999), with a ± of 50 N accuracy on cylindrical samples with nominal height of 40.0 mm and nominal diameter of 32.0 mm. Young's modulus is calculated from the linear strain.

**Table 1.** Sample codes of Batch 1 with different activators and the results from the reactivity test 1 and 2 of Batch 1. NS: No/not enough setting, NC: Not fully cured, C: cured, E: Efflorescence.

Sample Code	Composition	1	2	Sample Code	Composition	1	2
20Na0.5	20.00 g MK, 20.0 mL 0.5 M NaOH	NS	–	20Ca0.5	20.00 g MK, 0.74 g Ca(OH) <sub>2</sub> , 20.0 mL H <sub>2</sub> O	NC	–
15Na0.5	20.00 g MK, 15.0 mL 0.5 M NaOH	NS	–	15Ca0.5	20.00 g MK, 0.56 g Ca(OH) <sub>2</sub> , 15.0 mL H <sub>2</sub> O	NC	–
12.5Na0.5	20.00 g MK, 12.5 mL 0.5 M NaOH	C	NC	25Ca0.5	20.00 gr MK, 0.93 Ca(OH) <sub>2</sub> , 25.0 mL H <sub>2</sub> O	C	NC
20Na4	20.00 g MK, 20.0 mL 4 M NaOH	C	NC	25Ca1	20.00 gr MK, 1.85 Ca(OH) <sub>2</sub> , 25.0 mL H <sub>2</sub> O	NC	–
15Na4	20.00 g MK, 15.0 mL 4 M NaOH	C	C + E	30Ca1	20.00 gr MK, 2.22 g Ca(OH) <sub>2</sub> , 30.0 mL H <sub>2</sub> O	C	NC
12.5Na4	20.00 g MK, 12.5 mL 4 M NaOH	C	C + E	25Ca2	20.00 gr MK, 3.71 g Ca(OH) <sub>2</sub> , 25.0 mL H <sub>2</sub> O	NC	NC
20K0.5	20.00 g MK, 20.0 mL 0.5 M KOH	NS	–	30Ca2	20.00 gr MK, 4.45 g Ca(OH) <sub>2</sub> , 30.0 mL H <sub>2</sub> O	C	NC
15K0.5	20.00 g MK, 15.0 mL 0.5 M KOH	NS	–	25Ca3	20.00 gr MK, 5.56 g Ca(OH) <sub>2</sub> , 25.0 mL H <sub>2</sub> O	C	NC
12.5K0.5	20.00 g MK, 12.5 mL 0.5 M KOH	NC	–	30Ca3	20.00 gr MK, 6.67 g Ca(OH) <sub>2</sub> , 30.0 mL H <sub>2</sub> O	C	C
20K4	20.00 g MK, 20.0 mL 4 M KOH	NC	–	22.5Ca4	20.00 gr MK, 6.06 g Ca(OH) <sub>2</sub> , 22.5 mL H <sub>2</sub> O	C	C
15K4	20.00 g MK, 15.0 mL 4 M KOH	C	NC	25Ca4	20.00 gr MK, 7.41 g Ca(OH) <sub>2</sub> , 25.0 mL H <sub>2</sub> O	C	C
12.5K4	20.00 g MK, 12.5 mL 4 M KOH	C	NC	30Ca4	20.00 gr MK, 8.89 g Ca(OH) <sub>2</sub> , 30.0 mL H <sub>2</sub> O	C	C

**Table 2.** Sample codes of Batch 2 with Ca(OH)<sub>2</sub> de as activator and different aggregates.

Sample Code	Composition	Fillers
18MK30Ca4Q10	18.00 g MK, 8.89 g Ca(OH) <sub>2</sub> , 30.0 mL H <sub>2</sub> O	2.00 g Quartz sand M34
16MK30Ca4Q20	16.00 g MK, 8.89 g Ca(OH) <sub>2</sub> , 30.0 mL H <sub>2</sub> O	4.00 g Quartz sand M34
18MK30Ca4I10	18.00 g MK, 8.89 g Ca(OH) <sub>2</sub> , 30.0 mL H <sub>2</sub> O	2.00 g Inducal 105
16MK30Ca4I20	16.00 g MK, 8.89 g Ca(OH) <sub>2</sub> , 30.0 mL H <sub>2</sub> O	4.00 g Inducal 105
18MK30Ca4A10	18.00 g MK, 8.89 g Ca(OH) <sub>2</sub> , 30.0 mL H <sub>2</sub> O	2.00 g Ankerfill 125
16MK30Ca4A20	16.00 g MK, 8.89 g Ca(OH) <sub>2</sub> , 30.0 mL H <sub>2</sub> O	4.00 g Ankerfill 125

### 3 Results and discussion

Experiments were performed with Ca(OH)<sub>2</sub> as an activator for metakaolin-based geopolymers to investigate the reactivity and compare the results with more well-known activators. Subsequently, the basic physio-mechanical properties of Ca(OH)<sub>2</sub> activated metakaolin with low addition of aggregates were tested. The results of these tests are results from literature (Lubelli et al., 2019).

#### 3.1 Reactivity tests

The samples are visually evaluated and classed into three categories (Table 1). The first category is the sample is still fluid after 48 h, labelled as “no /not enough setting” (NS). In the second, the samples are pressable and labelled as “not fully cured” (NC). The last group is for completely hardened samples, labelled as cured (C). Samples with the lowest alkaline activator (0.5 M) do not cure, because there was too little reactivity to ensure cohesion in the sample (Alventosa et al., 2021).

The samples that cured during the first test are partially immersed in water to test if they remain their shape after 4 h (Table 1). Samples that fall apart after immersion are labelled “not cured” (NC). It means that the water from the activator evaporated too quickly without ensuring enough binding between the activator and the precursor. In Fig. 1 no. 12.5Na0.5, 20Na4, 15Na4, 12.5Na4, 15Ca0.5 and 25Ca0.5

are collapsing. Samples that remain their shape during exposure to water are labelled “cured” (C). It indicates binding between the precursor and the activator, as shown in Fig. 1 no. 22.5Ca4, 25Ca4 and 30Ca4. An additional label is given for efflorescence (E), which can be observed on the samples with NaOH as an activator (Fig. 2). This is physically and aesthetically undesired. Samples 30Ca3, 22.5Ca4, 25Ca4, 30Ca4 remain their shape and are selected for the next reactivity tests with CLSM and SEM. The samples with 20Na0.5, 15Na0.5, 12.5Na0.5, 20Na4, 15Na4, 12.5Na4, 20K4, 15K4 and 12.5K4 showed too little reactivity or efflorescence and were rejected for further testing.

In the last reactivity test phase the four selected samples (30Ca3, 22.5Ca4, 25Ca4, 30Ca4) will be evaluated with SEM-BSE on homogeneity and defects in the structure, like non-reacted and loose powder. In sample 30Ca3, 22.5Ca4 and 25Ca4 there is a lot of particles visible and microcracks can be observed. Although, some of the cracks and pores could also be related to the sample preparation. Sample 30Ca4 appears to be more blended and unified due to a stronger concentration of activator and also a larger amount of activator, which results in the forming of a gel and a higher degree of reaction. There are still particles visible, but less compared to sample 30Ca3 (Fig. 2).

The matrix of sample 30Ca4 is selected for the next recipes where different aggregates are added to the mixture in a 10 % and 20 % ratio. With SEM-BSE the different struc-



**Figure 1.** (a) Results from the second reactivity test, (b) detail picture of the efflorescence on the surface of 12.5Na4.

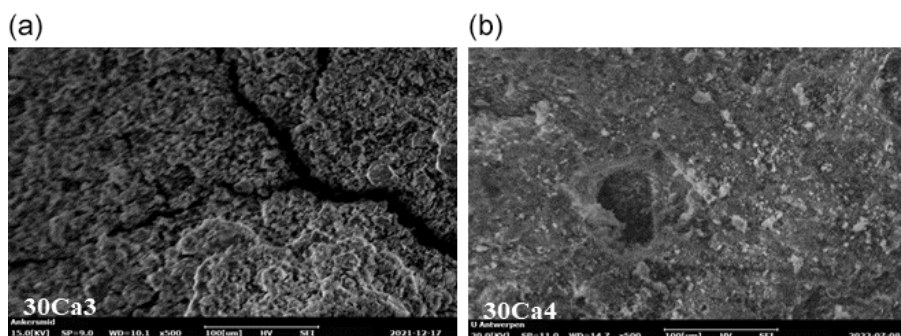


**Figure 2.** (a) SEM-BSE image of sample 30Ca3, (b) SEM-BSE image of sample 30Ca4.

tures of the samples with 10 % aggregates were made visible (Fig. 3). It should be noted that there was little difference with the samples with 20 %, because the ratio of aggregates is very low. The sample with 10 % sand (a) has an amorphous structure, it has homogeneous parts but also parts with a lot of particles and pores of all different sizes ( $\pm 10$ – $50 \mu\text{m}$ ). The sample with 10 % lime stone powder (b) is more homogeneous compared to the sample with 10 % sand (a). In addition, it shows very small pores combined with very large pores ( $\pm 75 \mu\text{m}$ ). The sample with 10 % marl powder (c) shows a structure with very large pores ( $\pm 200 \mu\text{m}$ ) and a lot of particles.

## 3.2 Mechanical properties

### 3.2.1 Open porosity and pore size distribution

The pore size distribution of sample 30Ca4 was measured with MIP (Fig. 4). The majority of pore range in size between 0.01 and  $0.5 \mu\text{m}$  diameter, which is typical for a AAM. This is probably due to a reaction between the metakaolin and the  $\text{Ca}(\text{OH})_2$  and not due to carbonatation of the calcium hydroxide. Provis (2018) mentions that adding calcium rich minerals could lead to pore-refining, which could explain the pore size of 30Ca4. Besides, Liu (2020) stated that the pore size decreases to  $0.03 \mu\text{m}$  by adding metakaolin to a lime mortar. There are similarities between 30Ca4 and the results of Longhi et al. (2020). The pore size of the alkali activated metakaolin activated with a 8 M NaOH solution it is between 0.01 and  $1 \mu\text{m}$ .

The open porosity of the samples is between 61 %–63 % (Table 3), which is very high. This is probably due to the low content of aggregates in the samples, so these numbers mainly give an image of the open porosity of the binders. The open porosity between 43.6 %–65.8 % of metakaolin-based geopolymers without aggregates of Longhi (2020) confirms this theory. Besides, Liu (2020) stated that the open porosity of a lime-mortar with metakaolin increases with 20 % compared to a lime-mortar without metakaolin, but it is still much lower than the results in this paper due to the added aggregates.

### 3.2.2 Water absorption

The capillary water absorption of the samples of Batch 2 is measured on four samples per recipe. The average of the capillary coefficient is shown in Table 3 and Fig. 5. The mass of almost all the different samples increased progressively up to around 16 h, and then slightly increased beyond this point from which the capillary moisture content is calculated. The saturation point of 30Ca4 is around 24 h, which is an exception. The samples with 10 % sand shifted the saturation point compared to 20 % sand. There is also a difference noticeable in the amount of water the samples can absorb. The samples with 10 % Ankerfill 125 and 10 % Inducal 105 absorb more compared to the samples with 20 %. However, this could also be the result of a horizontal internal crack in two out of four samples (which automatically lowers the average). One exception, the result of the sample with 10 % quartz sand is the exact opposite. The amount of water in the stone at the saturation point is shown in Table 4. The values differ between

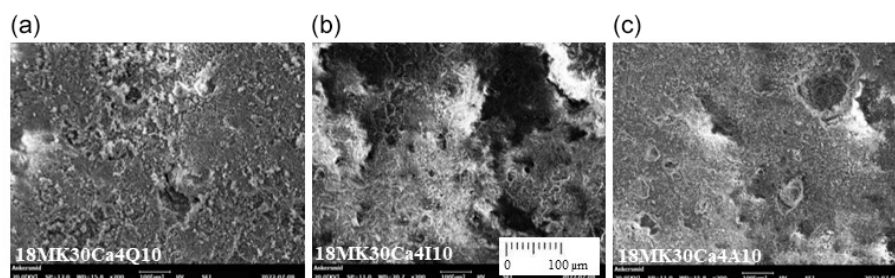


**Figure 3.** SEM-BSE image of sample 10 % quartz sand (a), 10 % marl powder (b), 10 % lime stone powder (c).

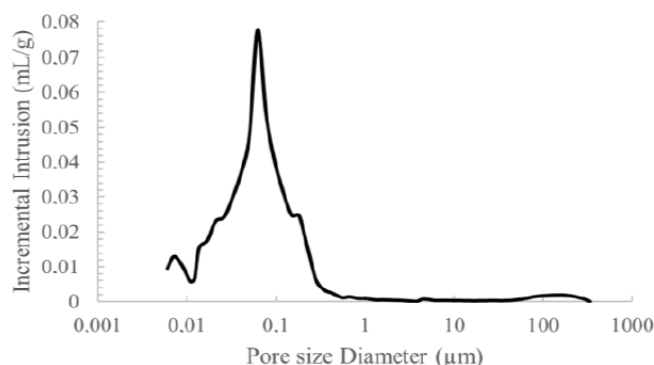


**Figure 4.** Pore size distribution of sample 30Ca4, showing a unimodal pore size distributed just below 0.1  $\mu\text{m}$ .

18.88 wt % (20 % marl powder) and 29.93 wt % (20 % quartz sand).

The capillary absorption coefficient is shown in Table 3. The sample with 10 % marl powder (Inducal 105) has the highest coefficient ( $104.10 \text{ g m}^{-2} \text{ s}^{-1/2}$ ). The sample with no aggregates 30Ca4 has the slowest capillary absorption. As quartz is a common used aggregate in repair mortars, the capillary absorption is mainly regulated by the binder. When comparing the results to those of typical repair mortars used in the Low Countries (Lubelli et al., 2019) it can be concluded that all the samples have a lower capillary absorption coefficient, hence being slower in capillary absorbing. This is most likely explained by the pore structure that is composed of fine pore throats distributed around 0.1  $\mu\text{m}$ , as was observed by MIP.

### 3.2.3 Bulk density

The bulk density of the samples lies between  $0.984 \text{ g cm}^{-3}$  (20 % quartz sand) and  $1.116 \text{ g cm}^{-3}$  (20 % marl powder, Inducal 105), see Table 3. These results are lower compared to repair mortars in the Low Countries (Benelux) (Lubelli et al., 2019) where the lowest results are  $1.350 \text{ g cm}^{-3}$  (highest  $2.303 \text{ g cm}^{-3}$ ). Also in comparison to similar metakaolin investigations (Van Deventer et al., 2009) ( $2.419$ – $2.962 \text{ g cm}^{-3}$ ), the acquired results are much lower. In comparison to the results of Hajjaji (2013),  $1.03$ – $1.11 \text{ g cm}^{-3}$ ,

the obtained results are similar. These geopolymers were designed using metakaolin and red mud as a source of aluminosilicate and no additional aggregates (Hajjaji et al., 2013). So the low ratio of aggregates could be a reason (a maximum of 20 %), and by having obtained a relative high open porosity of the binder (Table 3).

### 3.2.4 Compressive strength and Young's modulus

The uniaxial compressive strength and the Young modulus of the samples are displayed in Table 3. The compressive strength of all samples varies between 5.44 and 7.54 MPa and the Young's modulus differs between 0.150 and 0.216 GPa. Sample 30Ca4 has the highest compressive strength and the sample with 20 % marl powder (Inducal 105) has the highest Young's modulus. The samples with lime stone powder have the lowest strength, although the sample with 10 % Anker-fill 125 has the most homogeneous structure. The results are quite similar compared to typical repair mortars in the Low Countries (Lubelli et al., 2019). However, the amount of added aggregates in these tests are very low compared to Clausi et al. (2016a, b) ratio 1 : 1 (2016), so reaching higher strengths might be possible with adding larger amounts of aggregates.

## 4 Conclusions

A research into the use of  $\text{Ca(OH)}_2$  as an activator for metakaolin-based geopolymers and the effect of different aggregates on the properties of the samples is conducted. Reactivity tests showed a mixture of metakaolin and  $\text{Ca(OH)}_2$  slurry cures to a stable binder. These samples showed no efflorescence, in contrast to metakaolin samples activated with NaOH. Sample 30Ca4 has the most gel formation according to the SEM-BSE and it has a majority of pores between 0.01 and 0.5  $\mu\text{m}$ , similar to metakaolin-based geopolymers. Therefore it was selected to test the effect of different aggregates.

No negative effects on reactivity, density and porosity were observed when the aggregates were added. Although, the open porosity is relatively high, it is still comparable to other geopolymers without aggregates. The addition of ag-

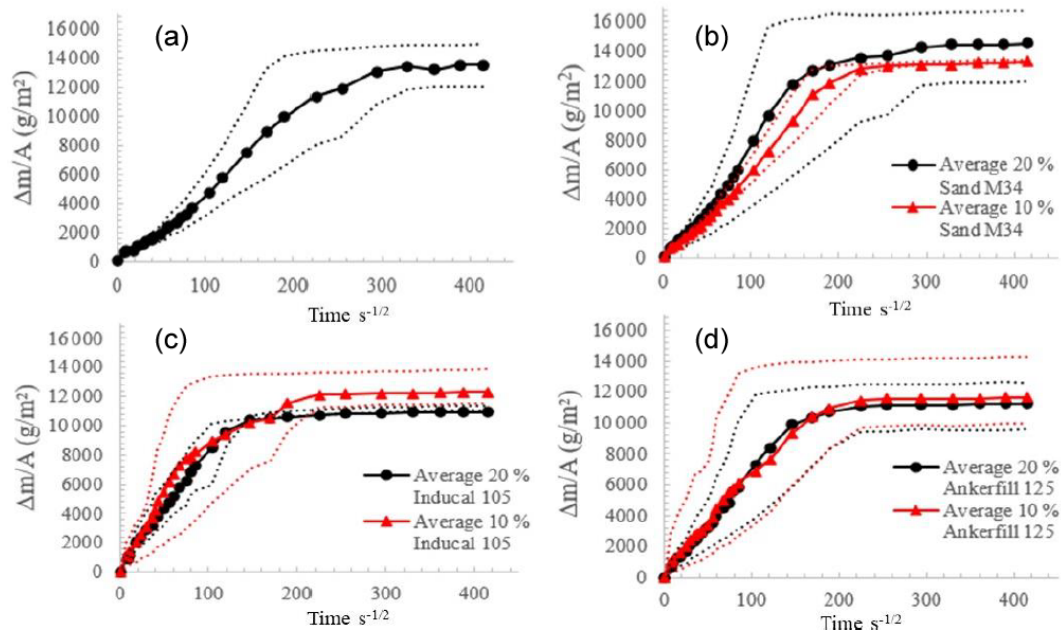


**Figure 5.** Capillary water absorption of the recipes (a) average “30Ca4”, (b) comparison Sand 10 % and 20 %, (c) comparison Inducal 105 10 % and 20 %, (d) comparison Ankerfill 125 20 % and 10 %. Dotted lines are minimum and maximum values.

**Table 3.** Physico-mechanical properties of Batch 2. C: capillary coefficient;  $\omega$ : capillary moisture content;  $W_{\text{atm}}$ : water absorption by immersion,  $\rho$ : bulk density; UCS: uniaxial compressive strength; E: Young’s modulus;  $\varphi$ : open porosity, by MIP.

Sample no.	C $\text{g m}^{-2} \sqrt{\text{s}}$ (min.–max.)	$\omega$ wt % (min.–max.)	$W_{\text{atm}}$ wt % (min.–max.)	$\rho$ $\text{g cm}^{-3}$ (min.–max.)	UCS MPa (min.–max.)	E GPa (min.–max.)	$\varphi$ vol %
30Ca4	52.47 (36.02–74.10)	25.93 (23.62–28.10)	33.21 (29.34–35.36)	1.00 (0.994–1.02)	7.540 (6.503–8.642)	0.207 (0.187–0.250)	62.91
18MK30Ca4Q10	64.15 (54.96–74.63)	27.25 (24.10–29.75)	31.26 (28.55–33.75)	1.004 (0.979–1.04)	6.639 (3.948–7.832)	0.186 (0.108–0.250)	63.74
16MK30Ca4Q20	83.31 (40.24–124.7)	29.93 (24.99–35.30)	34.27 (27.94–40.12)	0.984 (0.940–1.01)	6.292 (6.070–6.430)	0.202 (0.188–0.213)	64.27
18MK30Ca4I10	104.10 (48.58–163.7)	24.03 (19.41–27.72)	26.89 (22.42–30.80)	1.031 (0.985–1.07)	5.444 (3.948–6.171)	0.150 (0.108–0.180)	62.65
16MK30Ca4I20	81.72 (66.91–96.97)	18.88 (17.60–19.81)	22.45 (21.84–22.98)	1.116 (1.10–1.13)	7.034 (6.481–7.445)	0.216 (0.187–0.244)	61.32
18MK30Ca4A10	73.31 (43.72–131.6)	23.00 (19.78–29.04)	25.66 (21.44–32.61)	1.057 (1.03–1.08)	6.186 (5.360–6.837)	0.171 (0.137–0.194)	62.95
16MK30Ca4A20	73.50 (42.14–113.9)	21.58 (18.51–25.39)	24.64 (20.91–28.49)	1.078 (1.05–1.12)	5.604 (5.158–5.817)	0.154 (0.129–0.167)	63.36
Mortar based on zinc oxide [4]	275	6.3	–	2.303	19.54	0.006	20.5
Mortar based on Portland cement [4]	102	8.9	–	1.714	7.37	0.003	30.5



gregates increased the capillarity of the samples. Also, the mechanical strength decreased a little by adding the aggregates, but it is comparable to currently used repair mortars. These results showed the potential of using metakaolin and  $\text{Ca}(\text{OH})_2$  as a repair mortar for stone. However, if the low rate of water absorption mainly results from very small pore throats ( $< 1 \mu\text{m}$ ), a high water retention (low drying rate) could be an adverse effect, as well as its potential susceptibility to salt and ice crystallization stresses. Therefore, additional characterization of the physico-mechanical properties of the binder is desired, together with a further chemical characterization of the reaction products.

**Data availability.** The data are available by contacting the corresponding author.

**Author contributions.** The authors confirm contribution to the paper as follows: study conception and design: SvR, TDK and JB; data collection: SvR; analysis and interpretation of results: SvR, TDK and JB; draft manuscript preparation: SvR. All authors reviewed the results and approved the final version of the manuscript.

**Competing interests.** The contact author has declared that none of the authors has any competing interests.

**Disclaimer.** Publisher's note: Copernicus Publications remains neutral with regard to jurisdictional claims in published maps and institutional affiliations.

**Special issue statement.** This article is part of the special issue "European Geosciences Union General Assembly 2022, EGU Division Energy, Resources & Environment (ERE)". It is a result of the EGU General Assembly 2022, Vienna, Austria, 23–27 May 2022.

**Acknowledgements.** We express our thanks to Céline Thomachot-Schneider (Université de Reims Champagne-Ardenne), Julie Desarnaud (KIK-IRPA) and Jeroen Van Stappen (UGent) for their help with porosity measurements. We are grateful to Ing. Jan Stoop (UAntwerpen) for performing the uniaxial compressive strength tests.

**Financial support.** This research has been supported by the Universiteit Antwerpen (STIMPRO grant).

**Review statement.** This paper was edited by Michael Kühn and reviewed by Ana Teresa Lima and two anonymous referees.

## References

- Allali, F., Joussein, E., Indrissi Kandri, N., and Rossignol, S.: The influence of calcium content on the performance of metakaolin-based geomaterials applied in mortars restoration, *Material. Design*, 103, 1–9, <https://doi.org/10.1016/j.matdes.2016.04.028>, 2016.
- Alonso, S. and Palomo, A.: Calorimetric study of alkaline activation of calcium hydroxide-metakaolin solid mixtures, *Cement Concrete Res.*, 31, 25–30, [https://doi.org/10.1016/S0008-8846\(00\)00435-X](https://doi.org/10.1016/S0008-8846(00)00435-X), 2001.
- Alventosa, K. M. L. and White, C. E.: The effects of calcium hydroxide and activator chemistry on alkali-activated metakaolin pastes, *Cement Concrete Res.*, 145, 106453, <https://doi.org/10.1016/j.cemconres.2017.02.009>, 2021.
- Clausi, M., Magnani, L., Occhipinti, R., Riccardi, M., Zema, M., and Tarantino, S.: Interaction of Metakaolin-based geopolymers with natural and artificial stones and implications on their use in cultural heritage, *Int. J. Conserv. Sci.*, 7, 871–884, 2016a.
- Clausi, M., Tarantino, S., Magnani, L., Riccardi, M., Tedeschi, C., and Zema, M.: Metakaolin as a precursor of materials for applications in Cultural Heritage: Geopolymer-based mortars with ornamental stone aggregates, *J. Appl. Clay Sci.*, 132/133, 598–599, <https://doi.org/10.1016/j.clay.2016.08.009>, 2016b.
- Cong, P. and Cheng, Y.: Advances in geopolymer materials: A comprehensive review, *J. Traff. Trans. Eng.*, 8, 283–314, <https://doi.org/10.1016/j.jtte.2021.03.004>, 2021.
- Dimou, A. E., Metaxa, Z. S., Kourkoulis, S. K., Karatasios, I., and Alexopoulos, N. D.: Tailoring the binder matrix of lime-based binders for restoration interventions with regard to mechanical compatibility, *Constr. Build. Mater.*, 315, 125717, <https://doi.org/10.1016/j.conbuildmat.2021.125717>, 2022.
- EN 1015-11: European Standard, Methods of test for mortar for masonry – Part 11: Determination of flexural and compressive strength of hardened mortar, European Committee for Standardization (CEN), 1999.
- EN 1925:1999: European Standard, Natural stone test methods – Determination of water absorption coefficient by capillarity, European Committee for Standardization (CEN), 1999.
- EN 1936:2006: European Standard, Natural stone test methods – Determination of real density and apparent density, and of total and open porosity, European Committee for Standardization (CEN), 2007.
- Geraldes, C. F. M., Lima, A. M., Delgado-Rodrigues, J., Mimosa, J. M., and Pereira, S. R. M.: Geopolymers as potential repair material in tiles conservation, *Appl. Phys. A*, 122, 197, <https://doi.org/10.1007/s00339-016-9709-3>, 2016.
- Granizo, M. L., Alonso, S., Blanco-Varela, M. T., and Palomo, A.: Alkaline Activation of Metakaolin: Effect of calcium hydroxide in the products of reaction, *J. Am. Cer. Soc.*, 85, 225–231, <https://doi.org/10.1111/j.1151-2916.2002.tb00070.x>, 2002.
- Hajjaji, W., Andrejkovičá, S., Zanelli, C., Alshaaer, M., Dondi, M., Labrincha, J. A., and Rocha, F.: Composition and technological properties of geopolymers based on metakaolin and red mud, *Material. Design*, 52, 648–654, <https://doi.org/10.1016/j.matdes.2013.05.058>, 2013.
- Isebaert, A., Van Parys, L., and Cnudde, V.: Composition and Compatibility Requirements of Mineral Repair Mortars for Stone – A Review, *Constr. Build. Mater.*, 59, 39–50, <https://doi.org/10.1016/j.conbuildmat.2014.02.020>, 2014.

- Isebaert, A., Van Parys, L., Chudde, V., De Kock, T., and Baele, J. M.: Compatibility Assessment for Repair Mortars: An Optimized Cement-Based Mix for Tuffeau de Lincent, edited by: Hughes, J., Válek, J., and Groot, C., *Historic Mortars*, Springer, Cham, 169–184, [https://doi.org/10.1007/978-3-319-91606-4\\_13](https://doi.org/10.1007/978-3-319-91606-4_13), 2019.
- Liu, H., Wang, W., Zhao, Y., and Song, S.: Performance Evaluation of Lime Mortars with Metakaolin and CMC for Restoration Application, *J. Mater. Civ. Eng.*, 32, 10, [https://doi.org/10.1061/\(ASCE\)MT.1943-5533.0003377](https://doi.org/10.1061/(ASCE)MT.1943-5533.0003377), 2020.
- Longhi, M. A., Rodríguez, E. D., Walkley, B., Zhang, Z., and Kirchheim, A. P.: Metakaolin-based geopolymers: Relation between formulation, psychicochemical properties and efflorescence formation, *Composites Pt. B*, 182, 107671, <https://doi.org/10.1016/j.compositesb.2019.107671>, 2020.
- Lubelli, B., Nijland, T. G., van Hees, R. P. J.: Characterization and compatibility assessment of commercial stone repair mortars, 5th Historic Mortars Conference, 19–21 June 2019, Pamplona, Spain, 174–182, *Journal of Cultural Heritage*, <https://doi.org/10.1016/j.culher.2021.02.001>, 2019.
- Pacheco-Tornal, F., Labrincha, J. A., Leopelli, C., and Palomo, A., and Chindaprasart, P. (Eds.): *Handbook of Alkali-Activated Cements, Mortars and Concretes*, Woodhead Publishing Series in Civil and Structural Engineering, 54, ISBN: 9781782422761, <https://doi.org/10.1016/C2013-0-16511-7>, 2015.
- Pagnotta, S., Tenorio, A.L., Tinè, M. R., and Lezzerini, M.: Geopolymers as a potential material for preservation and restoration of Urban Build Heritage: an overview, *IOP Conf. Ser.-Earth Environ. Sci.*, 609, 012057, <https://doi.org/10.1088/1755-1315/609/1/012057>, 2020.
- Pereira, D. S T., Silva, F. J., Porto, A. B. R., Candido, V. S., Silva, A. C. R., Filho, F. D. C. G., and Monteiro, S. N.: Comparative analysis between properties and microstructures of geopolymeric concrete and portland concrete, *J. Mater. Res. Technol.*, 7, 606–611, <https://doi.org/10.1016/j.jmrt.2018.08.008>, 2018.
- Pouhet, R.: Formulation and durability of metakaolin-based geopolymers, *Civil Engineering*, Université Paul Sabatier – Toulouse III, NNT, 2015TOU30085, 2015.
- Provis, J. L.: Alkali-activated materials, *Cement Concrete Res.*, 114, 40–48, <https://doi.org/10.1016/j.cemconres.2017.02.009>, 2018.
- Ricciotti, L., Molino, A. J., Roviello, V., Chianese, E., Cennamo, P., and Roviello, G.: Geopolymer Composites for Potential Applications in Cultural Heritage, *Environments*, 4, 91, <https://doi.org/10.3390/environments4040091>, 2017.
- Siddique, R. and Klaus, J.: Influence of metakaolin on the properties of mortar and concrete: a Review, *Appl. Clay Sci.*, 43, 392–400, <https://doi.org/10.1016/j.clay.2008.11.007>, 2009.
- Van Deventer, J., Stephanus, J., and Provis, J. L.: *Geopolymers – Structure, Processing, Properties and Industrial Applications*, Woodhead Publishing, <https://doi.org/10.1533/9781845696382.1>, 2009.